Journal of Metals, Materials and Minerals, Vol.29 No.2 pp.37-41, 2019

Isothermal aging of Al-Ni-Sc alloy containing Al_3Ni microfibers and Al_3Sc nanoprecipitates

Chanun SUWANPREECHA[1,*], Jacques Perrin TOININ[2], Phromphong PANDEE[1], David C. DUNAND[2], and Chaowalit LIMMANEEVICHITR[2]

[1] *Department of Production Engineering, Faculty of Engineering, King Mongkut's University of Technology Thonburi, Bangkok 10140, Thailand*
[2] *Department of Materials Science and Engineering, Northwestern University, 2220 Campus Drive, Evanston, IL 60208, USA*

[*]**Corresponding author e-mail:** achanun.suwanpreecha@mail.kmutt.ac.th

Received date:
26 September 2018
Revised date:
16 February 2019
Accepted date:
8 March 2019

Keywords:
Al-Ni-Sc alloy
Atom probe tomography
Precipitation strengthening

Abstract

Binary Al-Sc alloys have excellent strength at room and elevated temperature up to 300°C due to coherent of Al_3Sc nanoprecipitates. Binary Al-Ni alloys are an alternative alloy for high-temperature applications owing to high-thermal stability of Al_3Ni microfibers. In this study, the hardness evolution at 300°C for up to 672 h for eutectic ternary Al-6Ni-0.4Sc (wt%) was studied and compared with binary Al-0.4Sc and Al-6Ni alloys. The Al-6Ni alloy maintains a constant hardness after aging at 300°C up to 672 h. Both Al-0.4Sc and Al-6Ni-0.4Sc alloys show strong precipitation strengthening response, with peak hardness reached after about 3 h aging, due to Al_3Sc precipitates. These precipitates were studied in Al-6Ni-0.4Sc via local electrode atom probe tomography and contain small amounts of Ni (0.04 at%) which do not affect the kinetics of precipitation. The microhardness evolution for Al-6Ni-0.4Sc can be explained through superposition of binary Al-0.4Sc and Al-6Ni alloys, indicating that both Al_3Sc nanoprecipitates and Al_3Ni microfibers contribute to strength

1. Introduction

Aluminum-Scandium (Al-Sc) alloys exhibit good mechanical properties at both room and elevated temperatures after being heat-treated to obtain a high number density of coherent Al_3Sc nanoprecipitates [1,2]. These precipitates have high thermal stability because of low diffusivity of Sc in Al [3] ($D_{Sc/Al} = 2.0 \times 10^{-17}$ m^2/s). The precipitates resist coarsening up to 300°C which is much higher than other precipitates in commercial age-hardenable alloys, such as Mg_2Si and Al_2Cu which rapidly coarsen at 150-200°C due to high diffusivity of Mg and Cu in aluminum ($D_{Mg/Al} = 1.1 \times 10^{-14}$ m^2/s, $D_{Cu/Al} = 1.8 \times 10^{-15}$ m^2/s) [4-6].

Eutectic aluminum-nickel casting alloys (Al-6.1 wt% Ni) are promising for high-temperature applications because of the high chemical and thermal stabilities of eutectic Al_3Ni fibers that can resist coarsening up to 400 °C [7-9]. Theses fibers have micron-scale length and submicron diameter, even for standard solidification. The Al_3Ni interface with the aluminum appears to be coherent thus increasing resistance to coarsening at high-temperature [10]. Moreover, the Al-Ni alloys have good castability and low tendency to hot tear resulting from the high volume fraction (~10 vol.%) of Al_3Ni microfibers [8].

In a previous study [7], we found that Al_3Sc precipitates formed in Al-6Ni-0.4Sc alloy during aging provide improved mechanical properties at both room and elevated temperature as compared to Sc-free Al-6Ni. The objective of the present study is to identify the effect of Sc addition in Al-6Ni alloy on the microhardness evolution by comparing with binary Al-0.4Sc and Al-6Ni alloys. This is achieved through microstructure imaging, Vickers microhardness measurement, and local electrode atom probe tomography (LEAP) after isothermal aging at 300°C.

2. Experimental procedures

Each of the three alloys - Al-0.4Sc, Al-6Ni, and Al-6Ni-0.4Sc (all in wt%) - was melted in a silicon carbide crucible using an induction furnace, using 99.9 wt% pure Al, Al-2 wt% Sc and Al-20 wt% Ni master alloys. The melt was degassed by Ar gas, cleaned by flux and then poured into a thick-wall cylindrical copper mold (90 mm outer diameter, 30 mm inner diameter, 70 mm height). The average cooling rate was 10°C/s. The chemical compositions were analyzed by spark emission spectroscopy and are shown in Table 1 (Si content is also reported due to the contamination from the SiC crucible). The specimens were cut from the cast ingot as quarter discs (15 mm in radius and 1.25 mm in thickness.) For microstructure analysis, the specimens were prepared by standard metallographic methods (polishing down to 1 μm diamond suspension) and imaged by field emission electron microscope (Hitachi SU8030 FE-SEM). The precipitate evolution was studied through isothermal aging in a muffle furnace in air at 300°C terminated by water quenching to room temperature.

DOI: 10.14456/jmmm.2019.16

The aged specimens were polished by standard metallographic methods (down to 1 µm diamond suspension) and subjected to Vickers microhardness tests (Struers Duramin 5 hardness tester) at least five times for each condition. Peak-aged Al-6Ni-0.4Sc was selected for study of the precipitates by LEAP. The specimen was shaped into a tip by focused-ion beam (FIB) with an in-situ lift out technique. A LEAP 4000X Si-X tomograph (Cameca, Madison, WI) [11,12] was used with a picosecond pulsed ultraviolet (wave length: 355 nm) laser at a pulse repetition rate of 500 kHz, a pulse energy of 30-50 pJ, and a tip temperature of 30 K. The three-dimensional tomographic data were analyzed by Cameca's integrated visualization and analysis software (IVAS).

Table 1. Alloy chemical compositions as determined by spark emission spectrometry

Nominal composition, wt%	Experimental composition, wt% (at%)			
	Ni	Sc	Si	Al
Al-0.4Sc	0* (0*)	0.44 (0.26)	0.12 (0.12)	Balance
Al-6Ni	5.95 (2.83)	0** (0**)	0.11 (0.11)	"
Al-6Ni-0.4Sc	6.04 (2.88)	0.42 (0.26)	0.10 (0.10)	"

* below detection limit of 100 wt. ppm
** below detection limit of 6 wt. ppm

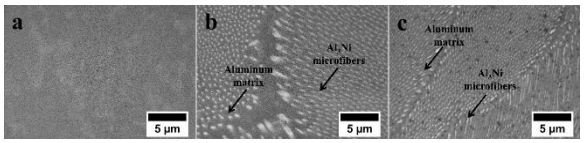

Figure 1. SEM micrographs of as-cast specimens: a) Al-0.4Sc, showing no sign of primary Al_3Sc phase, (b) Al-6Ni with Al_3Ni eutectic microfibers embedded in aluminum matrix and no primary Al_3Sc, and (c) Al-6Ni-0.4Sc, with similar structure as Al-6Ni.

3. Results and discussion

3.1 As-cast microstructure

The as-cast microstructures of the Al-0.4Sc, Al-6Ni, and Al-6Ni-0.4Sc alloys are shown in Figure 1(a), (b), and (c), respectively. For the Al-0.4Sc alloy (Figure 1(a)), the Sc content exceeded maximum solubility limit (~0.38 wt% at equilibrium). However, there is no sign of primary Al_3Sc. This is due to the high cooling rate of the copper mold, which maintains all Sc as super saturated solid solution. Thus, all available Sc can form Al_3Sc nanoprecipitates upon subsequent aging. The microstructure of the Al-6Ni (Figure 1(b)) and Al-6Ni-0.4Sc (Figure 1(c)) alloys are similar: Al_3Ni microfibers (bright contrast as arrowed in Figure 2 (b,c)) are embedded within the aluminum matrix (dark contrast as arrowed in Figure 1 (b,c)). Coarser Al_3Ni lamellae are found at the edge of the dendritic colonies [13]. Moreover, no other phases were found in Al-6Ni-0.4Sc (e.g., primary Al_3Sc particles). It can be seen that the addition of Sc into Al-6Ni does not significantly change the morphology of Al_3Ni microfibers, unlike in Al-Si alloys in which Sc can modify the plate-like eutectic Si to fine fibrous morphology [14].

3.2 Ambient-temperature hardness

Figure 2 shows Vickers microhardness evolution during isothermal aging at 300°C up to 672 h (~ 1 month). For Al-6Ni, the hardness remains constant throughout the experiment confirming the high thermal stability of Al_3Ni microfibers, which are known to resist coarsening up to 400°C [13,15]. For Al-0.4Sc, in the as-cast stage, the hardness is higher than that of pure Al (~200 MPa [16]), which is consistent with Al_3Sc nano-precipitation occurring on cooling after solidification. For Al-6Ni-0.4Sc, the hardness is significantly higher than for Al-0.4Sc in the as-cast stage, as expected from the strengthening of Al_3Ni microfibers. The evolutions of microhardness of Al-6Ni-0.4Sc and Al-0.4Sc are similar and can be divided into four stages: (1) incubation, where the hardness remains unchanged from the as-cast stage (< 0.5 h, probably ~0.1 h). (2) under-aging, where the hardness increases rapidly (~0.1 to ~3 h), (3) peak-aging, where the hardness reaches a plateau (~3 to 144 h), and (4) over-aging, where hardness slowly decreases (>144 h). The Al_3Sc precipitation kinetics (i.e., onset and duration of stages) during isothermal aging at 300°C appears to be unaffected by Ni additions. However, the hardness of Al-6Ni-0.4Sc is significantly higher than that of Al-0.4Sc, by ~ 300-400 MPa. The overall strength increment τ_t can be explained through superposition of two strengthening effects, from Al_3Ni microfibers and from Al_3Sc nanoprecipitates, as described by the empirical equation [17,18]:

$$\tau_t = (\sum_i (\tau_i^k))^{\frac{1}{k}} \quad (1)$$

where τ_i is the strength increment for a particular mechanism and the exponent k is between 1 (linear sum) and 2 (Pythagorean sum). This exponent was calculated by using increment in hardness (as compared to pure Al, 200 MPa). A good fit for Al-6Ni-0.4Sc is achieved with k = 1.39 (shown as a dashed-line in Figure 2). The k value is very close to k = 1.3 reported in Al-Sc-Zr alloys where $Al_3(Sc,Zr)$ nanoprecipitates coexist with Al_2O_3 submicron particles [19].

Table 2 Average compositions of Al_3Sc precipitate, matrix, and tip (at.%) for peak-aged Al-6Ni-0.4Sc (wt%), as determined by LEAP

	Composition (at.%)			
	Ni	**Sc**	**Si**	**Al**
matrix	0.020 ± 0.0003	0.008 ± 0.0002	0.018 ± 0.0003	99.953 ± 0.0004
tip	0.020 ± 0.0002	0.236 ± 0.0009	0.039 ± 0.0004	99.705 ± 0.001
precipitate	0.036 ± 0.0005	25.594 ± 0.121	2.002 ± 0.0388	72.368 ± 0.124

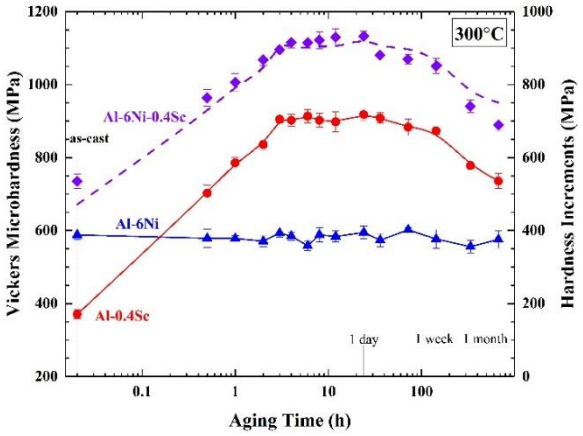

Figure 2 Evolution during isothermal aging of Al-0.4Sc, Al-6Ni, and Al-6Ni-0.4Sc. The dashed line curve for Al-6Ni-0.4Sc was calculated from Eq. (1) with k = 1.39 [20].

3.3 Local electrode atom probe tomography (LEAP)

The Al-6Ni-0.4Sc alloy at peak-aging (300°C, 24 h) was investigated by LEAP. The 3D LEAP reconstruction is shown in Figure 3. The tip contains part of an Al_3Ni microfiber shown in the left corner of the tip and numerous Al_3Sc precipitates visibly enriched with Si (present as clusters collocated with the Al_3Sc precipitates). However, there is no Ni cluster in the tip. The exact composition of the nanoprecipitates as measured by LEAP is calculated and reported in Table 2. Negligible Ni amounts (0.04 at.%) and substantial Si amounts (2 at.%) are present in the Al_3Sc nanoprecipitates. Thus, Ni not locked in the Al_3Ni microfibers partitions somewhat to the Al_3Sc precipitates, whose Ni content is twice that of the very low concentration found in the matrix. The low Ni amount present in the precipitates is consistent with the isothermal aging results showing that hardness is unaffected by Ni additions to the alloy. Silicon is known to accelerate Al_3Sc precipitation and can also increase the number density of precipitates. It also increases the thermodynamic driving force of Al_3Sc nanoprecipitates which can increase the precipitation kinetics. Moreover, Si also forms clusters acting as heterogeneous nucleation of the Al_3Sc precipitates, resulting in an increased nanoprecipitates number density [21-24]. However, in this study, the Si content in the Al-6Ni-0.4Sc alloy (~0.10 wt% Si) does not significantly differ from that in the Al-0.4Sc alloy (~0.12 wt% Si); therefore, the effects of Si on hardness increments and precipitation of Al_3Sc precipitates can be assumed to be the same in both alloys.

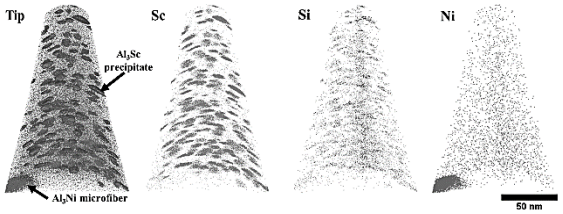

Figure 3. Atom-probe tomographic reconstruction of Al-6Ni-0.4Sc in the peak-aged condition (300°C/24 h). The tip contains part of an Al_3Ni microfiber shown in the lower left corner of the tip and numerous Al_3Sc nano-precipitates showing small amount of Si in their cores: Al atoms are shown in blue, Sc in red, Si in black, and Ni in green.

4. Conclusions

This study examines the effects of Sc addition in Al-6Ni alloy upon Al_3Sc precipitate evolution, with key results as follows:

1. The binary eutectic Al-6Ni alloy, which contains Al_3Ni microfibers, maintains its hardness up to 672 h upon aging at 300°C.
2. Sc addition (0.4 wt%) to Al-6Ni does not change the morphology of the Al_3Ni microfiber.
3. Ternary Al-6Ni-0.4Sc exhibits peak-aging at 300°C after 4 h, followed by over-aging after 144 h, due to Al_3Sc precipitation.
4. This hardness evolution at 300°C is similar to that of binary Al-Sc, indicating that Al_3Ni microfibers do not affect the evolution of the Al_3Sc precipitates, consistent with the very low Ni concentration (0.04 at.%) found in the Al_3Sc precipitates.
5. The hardness curve of Al-6Ni-0.4Sc at 300°C can be described *via* a superposition of the curves of Al-0.4Sc and Al-6Ni alloys, over the full aging time of 0-672 h, with a single best-fit exponent k = 1.39.

5. Acknowledgements

CS acknowledges the support of King Mongkut's University of Technology Thonburi through the "Petchra Pra Jom Klao Doctoral Scholarship" [Grant No. 01/2557]. Financial support from the "KMUTT 55th Anniversary Commemorative Fund" and the National

Research Council of Thailand are acknowledged. The authors sincerely thank Prof. David N. Seidman (Northwestern University) for useful discussions, and the use of Northwestern University Center for Atom Probe Tomography (NUCAPT). The LEAP tomograph at NUCAPT was purchased and upgraded with grants from the NSF-MRI (DMR-0420532) and ONR-DURIP (N00014-0400798, N00014-0610539, N00014-0910781, N00014-1712870) programs. NUCAPT received support from the MRSEC program (NSF DMR-1720139) at the Materials Research Center, the SHyNE Resource (NSF ECCS-1542205), and the Initiative for Sustainability and Energy (ISEN) at Northwestern University. DCD has financial interests relative to NanoAl, LLC, a company developing and marketing new aluminum alloys.

References

[1] D. G. E. L. S. Toropova, M. L. Kharakterova, and T. V. Dobatkina, *Advanced aluminum alloys containing scandium: structure and properties*, Gordon and Breach Science, Amsterdam 1998.

[2] D. N. Seidman, E. A. Marquis, and D. C. Dunand, Precipitation strengthening at ambient and elevated temperatures of heat-treatable Al(Sc) alloys, Acta Materialia 50(16) (2002) 4021-4035.

[3] S. I. Fujikawa, Impurity diffusion of scandium in aluminium, Defect and Diffusion Forum, Trans Tech Publ, 1997, pp. 115-120.

[4] F. Stadler, H. Antrekowitsch, W. Fragner, H. Kaufmann, and P.J. Uggowitzer, Effect of main alloying elements on strength of Al–Si foundry alloys at elevated temperatures, International Journal of Cast Metals Research 25(4) (2012) 215-224.

[5] F. J. Tavitas-Medrano, A. M. A. Mohamed, J. E. Gruzleski, F. H. Samuel, and H. W. Doty, Precipitation-hardening in cast AL–Si–Cu–Mg alloys, Journal of Materials Science 45(3) (2009) 641-651.

[6] Y. Du, Y. A. Chang, B. Huang, W. Gong, Z. Jin, H. Xu, Z. Yuan, Y. Liu, Y. He, and F. Y. Xie, Diffusion coefficients of some solutes in fcc and liquid Al: critical evaluation and correlation, Materials Science and Engineering: A 363(1–2) (2003) 140-151.

[7] C. Suwanpreecha, P. Pandee, U. Patakham, and C. Limmaneevichitr, New generation of eutectic Al-Ni casting alloys for elevated temperature services, Materials Science and Engineering: A.

[8] N. A. Belov, A. N. Alabin, and D. G. Eskin, Improving the properties of cold-rolled Al–6%Ni sheets by alloying and heat treatment, Scripta Materialia 50(1) (2004) 89-94.

[9] T. Koutsoukis and M. M. Makhlouf, Alternatives to the Al–Si Eutectic System in Aluminum Casting Alloys, International Journal of Metalcasting (2016) 1-6.

[10] Y. Fan and M. Makhlouf, The Al-Al3Ni Eutectic Reaction: Crystallography and Mechanism of Formation, Metallurgical and Materials Transactions A 46(9) (2015) 3808-3812.

[11] D. N. Seidman, Three-dimensional atom-probe tomography: Advances and applications, Annu. Rev. Mater. Res. 37 (2007) 127-158.

[12] T. F. Kelly and M. K. Miller, Atom probe tomography, Review of Scientific Instruments 78(3) (2007) 031101.

[13] C. S. Tiwary, S. Kashyap, D. H. Kim, and K. Chattopadhyay, Al based ultra-fine eutectic with high room temperature plasticity and elevated temperature strength, Materials Science and Engineering: A 639 (2015) 359-369.

[14] P. Pandee, C. M. Gourlay, S. A. Belyakov, R. Ozaki, H. Yasuda, and C. Limmaneevichitr, Eutectic Morphology of Al-7Si-0.3Mg Alloys with Scandium Additions, Metallurgical and Materials Transactions A 45(10) (2014) 4549-4560.

[15] Y. G. Nakagawa and G. C. Weatherly, The thermal stability of the rod Al3Ni-Al eutectic, Acta Metallurgica 20(3) (1972) 345-350.

[16] M. Handbook, vol. 2, Properties and Selection: Nonferrous Alloys and Special-Purpose Materials (1990) 713.

[17] E. A. Marquis, D. N. Seidman, and D. C. Dunand, Effect of Mg addition on the creep and yield behavior of an Al–Sc alloy, Acta Materialia 51(16) (2003) 4751-4760.

[18] U. Lagerpusch, V. Mohles, and E. Nembach, On the additivity of solid solution and dispersion strengthening, Materials Science and Engineering: A 319-321(Supplement C) (2001) 176-178.

[19] R. A. Karnesky, L. Meng, and D. C. Dunand, Strengthening mechanisms in aluminum containing coherent Al_3Sc precipitates and incoherent Al_2O_3 dispersoids, Acta Materialia 55(4) (2007) 1299-1308.

[20] C. Suwanpreecha, J. P. Toinin, R. A. Michi, P. Pandee, D. C. Dunand, and C. Limmaneevichitr, Strengthening mechanisms in AlNiSc alloys containing Al_3Ni microfibers and Al_3Sc nanoprecipitates, Acta Materialia 164 (2019) 334-346.

[21] D. Erdeniz, W. Nasim, J. Malik, A. R. Yost, S. Park, A. De Luca, N. Q. Vo, I. Karaman, B. Mansoor, D. N. Seidman, and D. C. Dunand, Effect of vanadium micro-alloying on the microstructural evolution and creep behavior of Al-Er-Sc-Zr-Si alloys, Acta Materialia 124 (2017) 501-512.

[22] A. De Luca, D. C. Dunand, and D. N. Seidman, Mechanical properties and optimization of the aging of a dilute Al-Sc-Er-Zr-Si alloy with a high Zr/Sc ratio, Acta Materialia 119 (2016) 35-42.

[23] O. Beeri, D. C. Dunand, and D. N. Seidman, Roles of impurities on precipitation kinetics of

dilute Al–Sc alloys, Materials Science and Engineering: A 527(15) (2010) 3501-3509.

[24] C. Booth-Morrison, Z. Mao, M. Diaz, D. C. Dunand, C. Wolverton, and D. N. Seidman, Role of silicon in accelerating the nucleation of Al_3(Sc,Zr) precipitates in dilute Al–Sc–Zr alloys, Acta Materialia 60(12) (2012) 4740-4752.